Synthesis and Characterization of the Atropisomeric Relationships of a Substituted *N*-Phenyl-Bipyrazole Derivative with Anti-inflammatory Properties

MARCIA P. VELOSO,[1,2,3] NELILMA C. ROMEIRO,[4] GILBERTO M.S. SILVA,[1,5,6] HÉLIO DE M. ALVES,[1] ANTONIO C. DORIGUETTO,[7] JAVIER ELLENA,[8] ANA L. P. MIRANDA,[1,5] ELIEZER J. BARREIRO[1,2,5] AND CARLOS A.M. FRAGA[1,2,5]*

[1]*Laboratório de Avaliação e Síntese de Substâncias Bioativas (LASSBio), Faculdade de Farmácia, Universidade Federal do Rio de Janeiro, Rio de Janeiro, RJ, Brazil*

[2]*Programa de Pós-Graduação em Química, Instituto de Química, Universidade Federal do Rio de Janeiro, RJ, Brazil*

[3]*Faculdade de Ciências Farmacêuticas, Universidade Federal de Alfenas, Alfenas, MG, Brazil*

[4]*Universidade Federal do Rio de Janeiro, Macaé, RJ, Brazil*

[5]*Programa de Pós-Graduação em Farmacologia e Química Medicinal, Instituto de Ciências Biomédicas, Universidade Federal do Rio de Janeiro, RJ, Brazil*

[6]*Instituto de Pesquisa Clínica Evandro Chagas, FIOCRUZ, Rio de Janeiro, RJ, Brazil*

[7]*Instituto de Ciências Exatas, Universidade Federal de Alfenas, Alfenas, MG, Brazil*

[8]*Instituto de Física de São Carlos, Universidade de São Paulo, São Carlos, SP, Brazil*

ABSTRACT This work describes the atropisomeric relationships of 3-methyl-5-(3-methyl-5-phenyl-1*H*-pyrazol-1-yl)-1-phenyl-1*H*-pyrazol-4-amine (**2d**), which belongs to series 4-aminobipyrazole derivatives designed as anti-inflammatory agents. The ^{1}H nuclear magnetic resonance spectra obtained in the presence of a chiral lanthanide shift salt associated to chiral high-performance liquid chromatography analysis, X-ray diffraction, and molecular modeling tools confirmed that *ortho* bis-functionalized bipyrazole **2d** exists as a mixture of *aR,aS*-atropisomers. These results provide useful information to understand the pharmacological profile of this derivative and of other 4-aminobipyrazole analogs. *Chirality 00:00–00, 2012.* © 2012 Wiley Periodicals, Inc.

KEY WORDS: bipyrazole; atropisomerism; axial chirality; nonsteroidal anti-inflammatory drugs; celecoxib; COX inhibitors

INTRODUCTION

Cyclooxygenase-2 (COX-2) is an enzyme involved in the production of prostaglandins associated with many important physiological and pathological states,[1] such as inflammation.[2] Selective COX-2 inhibitors,[3] for example, celecoxib (**1**),[4] have been shown to be potent anti-inflammatory agents with fewer side effects on the gastrointestinal (GI) tract and renal system than those of currently marketed nonselective nonsteroidal anti-inflammatory drugs,[5,6] in spite of some authors having described the cardiovascular side effects of other drugs belonging to this therapeutic class.[7]

In this context, as part of an ongoing research program designed to identify new anti-inflammatory drug candidates, a new series of *N*-phenylbipyrazole derivatives **2a-e** was designed (Fig. 1), synthesized, and pharmacologically assayed.[8] Based on these studies, we were able to identify the new anti-inflammatory prototype LASSBio-455 (**2c**), which displayed a moderate anti-edematogenic profile (Table S1, see Supplementary Material) without presenting GI toxicity. In addition, we have anticipated that the derivative **2d** could exist as a pair of atropisomers because of the presence of axial chirality resultant from the torsional barrier of the dihedral angle θ formed by N1–C5–N1–C5 atoms. Even for non-natural N,C-coupled heterobiaryl derivatives, atropisomerism studies have rarely been described in literature.[9,10]

Therefore, this article describes the synthesis and characterization of the atropisomeric relationships of the *N*-phenyl-bipyrazole derivative **2d** (Fig. 1), including the resolution and stereochemical assignment of its enantiomers.

MATERIALS AND METHODS

Chemistry

Melting points were determined with a Quimis 340M apparatus (Quimis, São Paulo, SP, Brazil) and are uncorrected. ^{1}H and ^{13}C nuclear magnetic resonance (NMR) spectra were determined in deuterochloroform containing approximately 1% tetramethylsilane as an internal standard with Brucker DRX200 spectrometer (Bruker, Billerica, MA, USA) at 200 and 50 MHz, respectively. Splitting patterns are as follows: s, singlet; d, doublet; br, broad; m, multiplet. ^{1}H and ^{13}C NMR assignments given for each compound were confirmed by heteronuclear multiple quantum correlation (HMQC) and heteronuclear multiple bon coherence (HMBC) experiments. Infrared (IR) spectra were obtained with a Nicolet-550 Magna spectrophotomer (Thermo Fisher Scientific Inc., West Palm Beach, Florida, USA) using KBr pellets. The mass spectra (MS) were obtained on GC/VG Micromass 12 spectrometer (VG Micromass Ltd., Manchester, UK) at 70 eV. Ultraviolet (UV) spectra were determined in a methanol solution on a Beckmann DU-70 spectrophotometer (Beckmann Coulter, Brea, CA, USA). Microanalysis data were obtained with a Perkin–Elmer 240 analyzer using a Perkin–Elmer AD-4 balance (Perkin-Elmer, Waltham, Massachusetts, USA). Before concentration under reduced pressure, all organic extracts were dried over anhydrous sodium sulfate powder. The progress of all reactions was monitored by thin-layer chromatography (TLC) performed on 2.0 × 6.0-cm aluminum sheets precoated with silica gel 60 (HF-254, Merck) to a thickness of 0.25 mm. The developed chromatograms were viewed under UV light at 254 nm.

Additional Supporting Information may be found in the online version of this article.

*Correspondence to: Carlos Alberto Manssour Fraga, LASSBio, Faculty of Pharmacy, Federal University of Rio de Janeiro, PO Box 68023, 21941-902 Rio de Janeiro, RJ, Brazil. E-mail: cmfraga@ccsdecania.ufrj.br

Received for publication 24 July 2011; Accepted 18 January 2012
DOI: 10.1002/chir.22016
Published online in Wiley Online Library (wileyonlinelibrary.com).

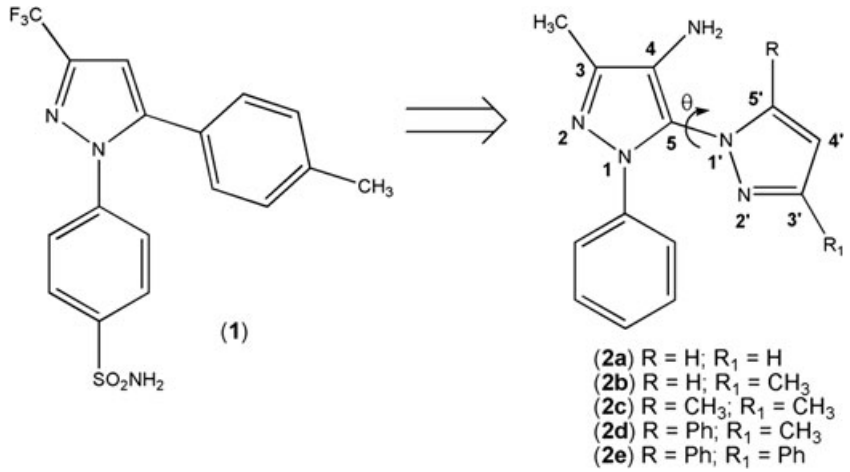

Fig. 1. New anti-inflammatory *N*-phenylbipyrazole derivatives (**2a–e**).

For column chromatography, Merck silica gel (70–230 mesh) was used. Solvents used in the reactions were dried, redistilled before use, and stored over +3–4 Å of molecular sieves. Reaction mixture was generally stirred under a dry nitrogen atmosphere.

*Preparation of 1-(3-Methyl-4-nitro-1-phenyl-1H-*pyrazol-5-yl) hydrazine (4)

To a solution of 5-chloro-3-methyl-4-nitro-1-phenyl-1*H*-pyrazole (**3**) (2.3 g, 9.6 mmol) in ethanol (15 ml), maintained under reflux, was added slowly 85% aq. hydrazine hydrate (1.9 ml), and the resulting mixture was heated at reflux for an additional 15 min. The reaction mixture was cooled, and the precipitate that formed was removed by filtration and crystallized from ethanol to give **4** (1.5 g, 68%), as an orange solid, mp. 150–151 °C; ^{1}H NMR (200 MHz, $CDCl_3$) δ 2.5 (s, 3H, $CH_{3\ Py}$), 3.5 (br, 2H, $NHNH_{2\ Py}$), 7.5 (m, 5H, $Phenyl_{Py}$), 8.0 (br, 1H, $NHNH_{2\ Py}$); ^{13}C NMR (50 MHz, $CDCl_3$) δ 14.6 ($3\text{-}CH_{3\ Py}$), 118.8 ($4\text{-}C_{Py}$), 125.2 ($2\text{-}C_{Ph}$, $6\text{-}C_{Ph}$), 128.7 ($4\text{-}C_{Ph}$), 129.3 ($3\text{-}C_{Ph}$, $5\text{-}C_{Ph}$, 140.0 ($1\text{-}C_{Ph}$), 146.6 ($5\text{-}C_{Py}$), 148.7 ($3\text{-}C_{Py}$); IR (KBr) cm^{-1}: 3348, 3331, 3233, and 3198 (N–H), 3060 (C–H_{arom}), 2995 and 2939 (C–H_{aliph}), 1649 and 1594 (δ N–H), 1535 (δ NO); MS (*m/z*): 233 (4%, M^+), 215 (43%), 170 (13%), 129 (53%), 104 (16%), 77 (100%); Anal. Calc. for $C_{10}H_{11}N_5O_2$: C, 51.50; H, 4.75; N, 30.03. Found: C, 51.67; H, 4.58; N, 29.99.

*Preparation of 3-Methyl-1-(3-methyl-4-nitro-1-phenyl-1H-*pyrazol-5-yl)-5-phenyl-1*H*-pyrazole (6d)

A mixture of hydrazine derivative **4** (1.0 g, 4.3 mmol) and benzoylacetone (**5d**) (4.3 mmol) in ethanol (10 ml) containing hydrochloric acid (1.0 ml) was heated at reflux for 1 h. The reaction mixture was poured onto cold water, producing a precipitate that was filtered and air-dried. The precipitate was crystallized from 50% aq. ethanol, yielding the desired bipyrazole derivative **6d** in 90% yield as pink crystals, mp. 113–114 °C; ^{1}H NMR (200 MHz, $CDCl_3$) δ 2.4 (s, 3H, $3\text{-}CH_{3\ Py}$), 2.6 (s, 3H, $3\text{-}CH_{3\ Py}$), 6.3 (s, 1H, $4\text{-}H_{Py}$), 6.8 (d, 2H, J = 8 Hz, $2''\text{-}H_{5Ph}$, $6''\text{-}H_{5Ph}$), 6.9 (d, 2H, J = 8 Hz, $2''\text{-}H_{1Ph}$, $6''\text{-}H_{1Ph}$), 7.3 (m, 6H, $3''\text{-}H_{5Ph}$, $4''\text{-}H_{5Ph}$, $5''\text{-}H_{5Ph}$, $3''\text{-}H_{1Ph}$, $4''\text{-}H_{1Ph}$, $5''\text{-}H_{1\text{-}Ph}$). ^{13}C NMR (50 MHz, $CDCl_3$) δ 14.0 ($3\text{-}CH_{3\ Py}$), 14.6 ($3\text{-}CH_{3\ Py}$), 107.9 ($4\text{-}C_{Py}$), 123.5 ($2''\text{-}C_{1Ph}$, $6''\text{-}C_{1Ph}$), 126.2 ($4\text{-}C_{Py}$), 127.4 ($2''\text{-}C_{[5Ph}$, $6''\text{-}C_{5Ph}$), 128.7 ($3''\text{-}C_{1Ph}$, $5''\text{-}C_{1Ph}$), 129.0 ($4''\text{-}C_{1Ph}$), 129.1 ($4''\text{-}C_{5\ Ph}$), 129.3 ($3''\text{-}C_{5Ph}$–$5''\text{-}C_{5Ph}$), 129.6 ($1''\text{-}C_{1Ph}$), 135.4 ($5\text{-}C_{Py}$), 137.0 ($1''\text{-}C_{5\ Ph}$), 146.8 ($3\text{-}C_{Py}$), 147.8 ($5\text{-}C_{Py}$), 153.1 ($3\text{-}C_{Py}$). IR (KBr) cm^{-1}: 3060 and 3003 (C–H_{arom}); 2962 and 2923 (C–H_{aliph}); 1603 and 1586 (δ N-H); 1599 (CC); 1435 and 1364 (δ NO). Anal. Calc. for $C_{20}H_{17}N_5O_2$: C, 66.84; H, 4.77; N, 19.49. Found: C, 67.03; H, 4.88; N, 19.55.

*Preparation of 3-Methyl-5-(3-methyl-5-phenyl-1H-*pyrazol-1-yl)-1-phenyl-1*H*-pyrazol-4-amine (2d)

A mixture of nitro-bipyrazole derivative **6d** (3.7 mmol), iron powder (0.01 g, 20.8 mmol), and NH_4Cl (0.1 g, 2.2 mmol) in 7.3 ml de EtOH:H_2O (2:1) was heated at reflux for 1 h. The hot mixture was filtered through Celite and concentrated in vacuum. The residue was diluted with H_2O and extracted with EtOAc (5 × 30 ml). The EtOAc layer was dried over anhydrous Na_2SO_4 and concentrated to give the corresponding amino derivative **2d** obtained in 98% yield, as clear orange oil. ^{1}H NMR (300 MHz, $CDCl_3$) δ 2.3 (s, 3H, $3\text{-}CH_{3\ Py}$), 2.4 (s, 3H, $3\text{-}CH_{3\ Py}$), 3.0 (br, 2H, $NH_{2\ Py}$), 6.3 (s, 1H, $4\text{-}H_{Py}$), 6.7 (d, 2H, J = 8 Hz, $2''\text{-}H_{5Ph}$, $6''\text{-}H_{5Ph}$), 6.9 (d, 2H, J = 8 Hz, $2''\text{-}H_{1Ph}$, $6''\text{-}H_{1Ph}$), 7.1 (m, 6H, $3''\text{-}H_{1Ph}$, $4''\text{-}H_{1Ph}$, $5''\text{-}H_{1Ph}$, $3''\text{-}H_{5\ Ph}$, $4''\text{-}H_{5Ph}$, $5''\text{-}H_{5Ph}$). ^{13}C NMR (75 MHz, $CDCl_3$) δ 11.3 ($3\text{-}CH_{3\ Py}$), 13.6 ($3\text{-}CH_{3\ Py}$), 106.5 ($4\text{-}C_{Py}$), 121.4 ($2''\text{-}C_{1Ph}$, $6''\text{-}C_{1Ph}$), 125.4 ($5\text{-}C_{Py}$), 125.9 ($4\text{-}C_{Py}$, $4''\text{-}C_{1Ph}$), 127.0 ($2''\text{-}C_{5Ph}$, $6''\text{-}C_{5Ph}$), 128.1 ($3''\text{-}C_{5Ph}$, $5''\text{-}C_{5Ph}$), 128.4 ($3''\text{-}C_{1Ph}$, $5''\text{-}C_{1Ph}$), 129.6 ($1''\text{-}C_{5Ph}$), 138.2 ($1''\text{-}C_{1Ph}$), 139.2 ($3\text{-}C_{Py}$), 146.6 ($5\text{-}C_{Py}$), 151.0 ($3\text{-}C_{Py}$); IR (KBr) cm^{-1}: 3388, 3295, 3206, and 3129 (N-H), 3068 (C-H_{arom}), 2962 and 2927 (C-H_{aliph}), 1642 and 1595 (δ N-H), 1502 (CC); UV (MeOH), λ, nm (log ε): 210 (4.22), 246 (4.12); Anal. Calc. for $C_{20}H_{19}N_5$: C, 72.93; H, 5.81; N, 21.26. Found: C, 73.12; H, 5.78; N, 21.10.

A thorough description of the 4-nitrobipyrazole (**6a**, **6b**, **6c**, and **6e**) and 4-aminobipyrazole (**2a**, **2b**, **2c**, and **2e**) synthesis can be found in the Supplementary Material.

*Preparation of 1-(3-Methyl-5-(3-methyl-5-phenyl-1H-*pyrazol-1-yl)-1-phenyl-1*H*-pyrazol-4-yl)-3-((*R*)-1-(naphthalen-2-yl)ethyl)urea (7a,b)

A mixture of 3-methyl-5-(3-methyl-5-phenyl-1*H*-pyrazol-1-yl)-1-phenyl-1*H*-pyrazol-4-amine (**2d**) (3 mmol), (*R*)-(−)-ethyl-1-(1-naphthyl)-isocyanate (0.59 g, 3 mmol), and triethylamine (0.91 g, 9 mmol) dissolved in 5 ml of tetrahydrofuran (THF) was stirred at room temperature on N_2 atmosphere for 15 min. The THF was removed under reduced pressure, and the reaction mixture was poured in water and the precipitate collected by filtration and dried to give 96% of urea derivative **7a,b** as a brown solid, mp 139–140 °C. ^{1}H NMR (300 MHz, $CDCl_3$) δ 1.3 (dd, 3H, J = 5.1 Hz, CH-CH_3 [a]), 1.6 (dd, 3H, J = 5.0 Hz, CH-CH_3 [b]), 2.1 (s, 6H, $3\text{-}CH_3$-Py [a + b]), 2.2 (s, 3H, $3\text{-}CH_3$-Py [a]), 2.4 (s, 3H, $3\text{-}CH_3$-Py [b]), 3.7 (q, 1H, J = 5.1 Hz, CH-CH_3 [b]), 4.1 (q, 1H, J = 5.1 Hz, CH-CH_3 [b]), 5.7 (s, 1H, 4-H-Py [a]), 5.8 (s, 1H, 4-H-Py [b]), 6.1 (br, 1H, NH_2-Py [a]), 6.2 (br, 2H, NH_2-Py [b] + NHCO [a]), 6.7 (br, 1H, NHCO [b]), 7.1 (m, 17H, 2″-H-[5-Ph]–6″-H-[5-Ph], 2″-H-[1-Ph]–6″-H-[1-Ph], 1-H-Naph–7-H-Naph [a]), 7.3 (m, 17H, 2″-H-[5-Ph]–6″-H-[5-Ph], 2″-H-[1-Ph]–6″-H-[1-Ph], 1-H-Naph–7-H-Naph [b]); ^{13}C NMR (75 MHz, $CDCl_3$) δ 12.0 and 12.5 ($3\text{-}CH_3$-Py), 13.5 and 13.7 ($3\text{-}CH_3$-Py), 24.1 and 25.0 (CHCH_3), 47.7 and 49.6 (CHCH_3), 107.3 and 107.5 (4″-C-Py), 109.5 109.0 (4-C-Py), 124.0 124.3 (8-Naph), 124.1 124.5 (2″-C-[1-Ph]–6″-C-[1-Ph]), 124.4 124.7 (7-Naph), 125.1 125.5 (3-Naph), 125.3 125.8 (4-Naph), 126.2 126.7 (5-Naph), 126.5 126.9 (2″-C-[5-Ph]–6″-C-[5-Ph]), 126.9 127.1 (1-Naph), 127.6 127.8 (6-Naph), 128.1 128.5 (4″-C-[5-Ph]), 128.7 129.0 (5-C-Py), 129.1 129.4 (3″-C-[1-Ph]–5″-C-[1-Ph]), 129.9 130.2 (3″-C-[5-Ph]–5″-C-[5-Ph]), 130.5 130.7 (4-C-[1-Ph]), 131.5 131.9 (1″-C-[5-Ph]), 135.0 135.3 (1″-C-[1-Ph]), 139.6 140.2 (2-Naph), 142.6 142.9 (5-C-Py), 145.6 145.7

(3-C-Py), 148.3 148.4 (3-C-Py); 151.6 152.0 (CO). Anal. Calc. for $C_{33}H_{30}N_6O$: C, 75.26; H, 5.74; N, 15.96. Found: C, 75.49; H, 5.72; N, 16.03.

High-Performance Liquid Chromatography Analysis

A Lachrom high-performance liquid chromatography (HPLC) system Merck equipped with a model D7000 interface, an L-7100 pump, an L-7450A diode array detector (DAD), and an L-7612 solvent degasser was used. The injections were performed manually with a Rheodyne injector (IDEX Health & Science, Oak Harbor, WA, USA) valve equipped with a 20-μl sample loop. Data were analyzed using Multi-Hauser Mixed Standard software supported on a Compaq Pentium II 250 MHz computer. A Lichosorb (N. 738342) RP-18 column (250 mm × 4 mm × 5 μm) was coupled to a Lichrocart 25-4 HPLC guard column cartridge. The chromatographic analyses were run with acetonitrile and water (adjusted to pH 3 with trifluoroacetic acid (TFA) 0.1%) gradients. The sample elution was carried out using a liner gradient of acetonitrile/water (taken to pH 3 with 0.1% of trifluoroacetic acid) from 20:80 to 80:20 over 20 min, and then to 100% acetonitrile over 1 min, followed by isocratic elution with acetonitrile for 5 min. The mobile phase was returned to its initial proportion and the column was equilibrated for 5 min. The analysis time was about 15 min, and the flow rate was constant at 1.0 ml/min. UV detection was performed using DAD in the range 210–350 nm to resolve most of the constituents. Integration parameters were used from 5 to 30 min to avoid interference of the solvents.

For chiral HPLC analysis, we have used a Regis (S,S) Whelk-O 1, 5 μm, 100 Å (25 cm × 4.6 mm i.d.) column, and the samples were eluted with a mixture of *n*-hexane/ethyl acetate (60:40). UV detection was performed at 250 nm.

The solvents used were of HPLC grade purchased from Tedia (Tedia Brazil, Rio de Janeiro, RJ, Brazil). Solvents were filtered through a Millipore filter (0.45 μm) and degassed in an ultrasonic bath (Thornton model T28220) for 10 min before use.

X-Ray Experiment

A well-shaped single crystal was chosen for the X-ray experiment. The measurement was made at 120 K on an Enraf–Nonius Kappa-CCD diffractometer (Bruker AXS, Inc., Madison, WI, USA) with graphite monochromated Mo Kα. Data were collected up to 50° in 2θ, with a redundancy of 4. The final unit cell parameters were based on all reflections. The temperature was controlled using an Oxford Cryosystem low temperature device. Data collection was made using the *COLLECT* software;[11] integration and scaling of the reflections were performed with the HKL Denzo–Scalepack software system.[12] Absorption corrections were carried out using the multiscan method.[13] The structures were solved with SHELXS-97.[14] The model was refined using SHELXL-97.[15] The H atoms of the phenyl and methyl groups were positioned stereochemically and were refined with fixed individual displacement parameters [Uiso(H) = 1.2Ueq($C_{aromatic}$) or 1.5Ueq($C_{methoxy}$)] using the SHELXL riding model with C–H length ranging from 0.93 to 0.98 Å. The hydrogen bond to N(1) atom (Fig. 6) was found in successive difference Fourier maps. Its fractional coordinates and isotropic thermal displacement were allowed to vary during the refinement. WINGX software was used to analyze and prepare the data for publication.[16] Crystal data, data collection procedures, structure determination methods, and refinement results are summarized in Table 2.

Crystallographic data for the structural analysis for the complexes discussed here have been deposited at the Cambridge Crystallographic Data Centre, 12 Union Road, Cambridge CB2 1EZ, UK, and are available on request, quoting the deposition number CCDC 817208.

Computational Methods

In this work, semi-empirical optimizations were carried out using the AM1[17] method with the Spartan for Linux '08 software package.[18] AM1 results were used as input for the ab initio molecular orbital calculations, which were carried out using Spartan '08. Restricted Hartree–Fock calculations with the split-valence 6-31G* basis set, which includes a set of d-type polarization functions on all nonhydrogen atoms, were used.[19] Single point energy calculations at HF/6-31G* level were used to evaluate the order of stability of atropisomers. Conformational analysis of compound 1a has been undertaken in Spartan '08[2] using the dihedral defined by C1–C2–N3–N4 (Fig. 7), which has been rotated systematically by 10°.

TABLE 2. Crystal data and structure refinement for atropisomeric bipyrazole derivative 2d

Empirical formula	$C_{20}H_{19}N_5$
Formula weight	329.40
Temperature	120(2) K
Wavelength	0.71073 Å
Crystal system	Monoclinic
Space group	$P2_1/c$
Unit cell dimensions	a = 9.0950(4) Å, b = 10.4050(5) Å c = 18.8545(9), β = 99.485(3)
Volume	1759.9(1) Å^3
Z	4
Density (calculated)	1.243 Mg/m^3
Absorption coefficient	0.077 mm^{-1}
Crystal size	0.20 × 0.08 × 0.05 mm^3
Theta range for data collection	2.94° to 25.00°
Reflections collected	10 221
Independent reflections	3086 [R(int) = 0.0482]
Completeness to θ = 25.00°	99.4%
Refinement method	Full-matrix least-squares on F^2
Data/restraints/parameters	3086/0/235
Goodness-of-fit on F^2	1.028
Final R indices [$I>2\sigma(I)$]	R1 = 0.0498, wR2 = 0.1291
R indices (all data)	R1 = 0.0620, wR2 = 0.1402
Extinction coefficient	0.046(7)
Largest diff. peak and hole	0.345 and −0.278 e.Å^{-3}

RESULTS AND DISCUSSION

Chemistry

The planned synthetic route to achieve the new derivative **2d** and other analogs exploited as raw material 5-chloro-3-methyl-4-nitro-1-phenylpyrazole **3**[20] previously used in our research group in the synthesis of bioactive antiplatelet[21] and anticholinesterase[22] agents (Scheme 1). This easily accessible compound was used to obtain the corresponding hydrazine derivative **4**, in 68% yield, by nucleophilic displacement of the chlorine atom at C-5 of **3** with hydrazine hydrate. The pyrazolyl-hydrazine derivative **4** was subsequently used in the regioselective construction of the second pyrazole ring

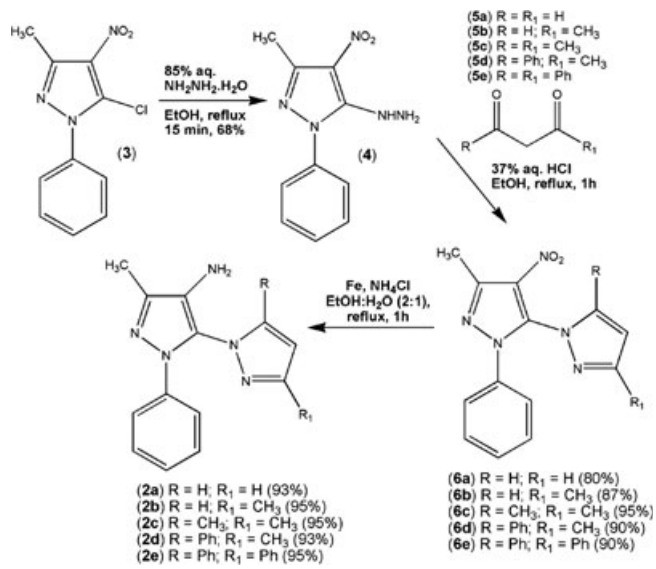

Scheme 1. Synthetic route used for the preparation of bipyrazole derivative **2a–e**.

present at C-5 of **2a–e**, through its condensation with the appropriate 1,3-dicarbonyl compound (**5**), furnishing, respectively, the desired 4-nitro-1,5-bipyrazole derivative **6a–e**, in yields ranging from 80% to 95%. Compounds **6a–e** presented structural patterns in agreement with what has been previously described.[20] Finally, the introduction of the pharmacophoric amino subunit at C-4 of the central heteroaromatic ring of the target compound **2a–e** was achieved in 93–95% yield by using activated iron powder in aqueous ethanol at reflux to reduce the nitro group of the corresponding derivative **6a–e**.[23]

Determination of the Atropisomerism Using Nuclear Magnetic Resonance and High-Performance Liquid Chromatography as Tools

The characterization of the atropisomerism of *N*-phenylbipyrazole derivative **2d** began with the analysis of its ^{1}H-NMR chemical shifts using different concentrations (0.005 to 0.1 M) of ytterbium tris[3-(heptafluoropropylhydroxymethylene)-(+)-camphorate] as chiral lanthanide salt,[16,24] which can be coordinated with the amino group at C-4, promoting different stereoelectronic effects in functional groups of the atropisomers of **2d**. In fact, we were able to identify a clear duplication of the signals referent to the hydrogens of the two methyl groups at C-3 and C-3 of **2d**, which appeared, in the ^{1}H-NMR spectrum without addition of (+)-Yb(hfc)$_3$, as singlet signals in δ 2.39 and 2.29 ppm, respectively (Fig. 2A). These results are in agreement with the hypothesis that **2d** exists as a mixture of enantiomers that are able to form diastereomeric complexes with the chiral lanthanide salt. Moreover, it can be observed that hydrogens of C-3 attached methyl group showed a major difference in the chemical shift (Table 1), after the subsequent increase of the molar concentration of the ^{1}H-NMR shift salt, because of a great stereospatial influence in the rotation of sigma bond between the two pyrazole rings, confirming the existence of the atropisomers of **2d**.

In addition, to confirm the NMR results previously evidenced, we performed an HPLC analysis of the atropisomeric mixture of **2d** using a chiral stationary phase supported in an analytical (S,S)-Whelk-O 1 column,[25] using a mixture of *n*-hexane/AcOEt (60:40) as eluent. Under those conditions, we were able to detect two UV absorptions at 250 nm with retention time of 2.96 and 6.80 min, corresponding to the enantiomeric pair of atropisomers of **2d** (Fig. 3). Despite that we have separated the atropisomers of **2d** by using this analytical procedure, under the experimental conditions developed, we were not able to obtain sufficient amount of the pure atropisomers to perform the determination of their biological activity, even after several consecutive runs. The obtained samples contained at least 5% of each other atropisomer, probably because of their partial configurational instability.

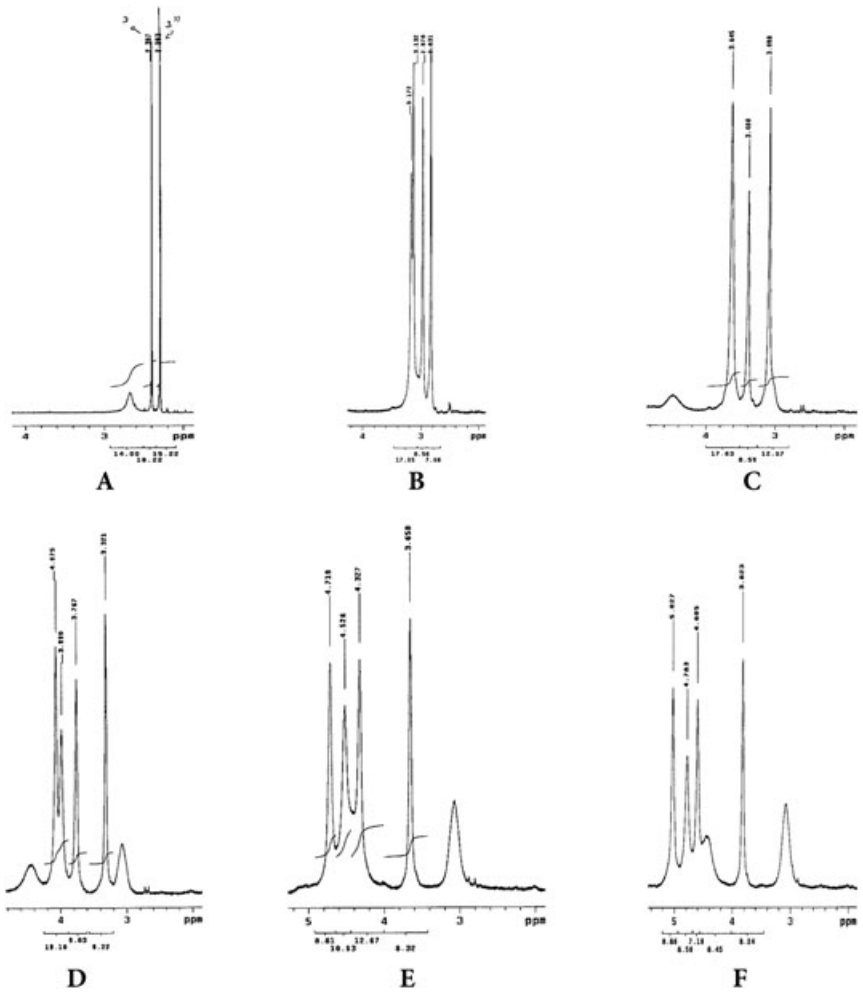

Fig. 2. ^{1}H-NMR spectra of the bipyrazole derivative **2d** with variant concentrations of Yb(thc)$_3$. **(A)** No addiction; **(B)** addition of Yb(thc)$_3$ (0.005 M); **(C)** addition of Yb(thc)$_3$ (0.010 M); **(D)** addition of Yb(thc)$_3$ (0.025 M); **(E)** addition of Yb(thc)$_3$ (0.050 M); **(F)** addition of Yb(thc)$_3$ (0.1 M) (Table 1).

TABLE 1. Chemical shifts of the methyl hydrogens of the derivative 2d in the absence or in the presence of (+)-Yb(thc)$_3$

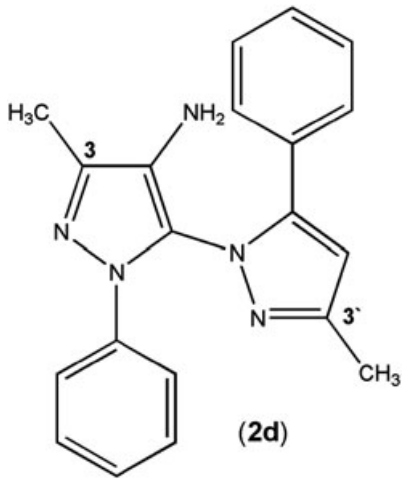

Entry	Concentration Yb(thc)$_3$ (M)[1]	CH_3-3-C			CH_3-3-C		
		δ_A (ppm)	δ_B (ppm)	δ[2]	δ_A (ppm)	δ_B (ppm)	δ
1	0	2.39		0	2.29		0
2	0.005	2.83	2.97	0.14	3.13	3.17	0.04
3	0.010	3.09	3.40	0.40	3.64	3.64	0.00
4	0.025	3.32	3.76	0.44	3.99	4.07	0.08
5	0.050	3.65	4.32	0.67	4.52	4.71	0.19
6	0.100	3.82	4.60	0.78	4.78	5.02	0.24

[1]All experiments were made at room temperature in a Brucker DRX200 spectrometer operated at 200 MHz.
[2]$\delta = \delta_B - \delta_A$.

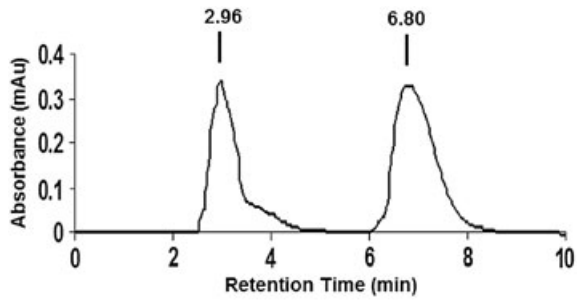

Fig. 3. Chiral HPLC analysis of atropisomeric mixture of *N*-phenylbipyrazole derivative **2d**.

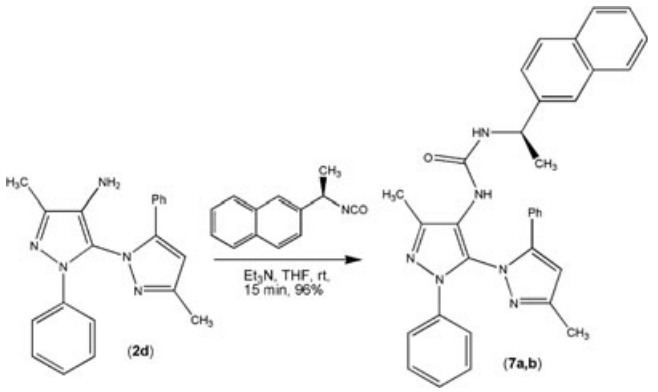

Scheme 2. Synthesis of diastereomeric bipyrazole urea derivatives **7a,b**.

In spite of our previous results having strongly indicated the presence of a mixture of the atropisomers of the *N*-phenyl-bipyrazole derivative **2d**, we decided to promote its derivatization to the corresponding mixture of diastereomeric ureidic derivatives **7a,b** through the reaction with (*R*)-(−)-ethyl-1-(1-naphthyl)-isocyanate and triethylamine in THF (Scheme 2). The diastereomeric mixture of the R,M and R,P urea derivatives **7a** and **7b** was obtained in 96% yield and characterized by the analysis of its ^{1}H- and ^{13}C-NMR spectra (see Materials and methods section), which presented duplicated signals relative to the hydrogen at the chiral center of **7a,b**, in agreement with the presence of two diastereomers. Moreover, reversed-phase HPLC analysis of the mixture **7a,b** confirmed this evidence, through the presence of two peaks with retention times of 9.81 and 10.72 min (Fig. 4), after elution with a mixture of acetonitrile/water adjusted to pH 3.

X-Ray Analysis

The crystal structure of **2d** was determined in space group $P2_1/c$ (Table 2). This is an important result taking into account that the initial motivation to perform the X-ray diffraction study arose from the possible atropisomerism of **2d**, as identified by NMR and HPLC techniques. Considering the restrictions on the formation of chiral and achiral crystal structures from chiral or achiral molecules,[26,27] an enantiomerically pure chiral molecule is not allowed to crystallize in a centrosymmetric space group. On the other hand, racemates of chiral molecule are permitted to crystallize either in achiral or chiral structures. Therefore, because **2d** is a chiral molecule crystallized in a centrosymmetric space group ($P2_1/c$), it is a crystalline racemate in which the two atropisomers (P/M: 50/50) are present in equal amounts in

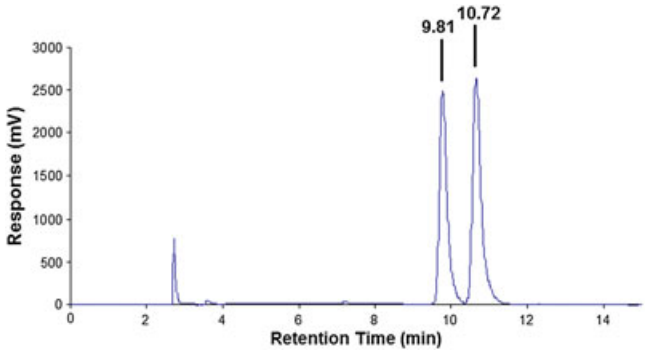

Fig. 4. Reversed-phase HPLC analysis of the diastereomeric mixture of *N*-phenylbipyrazole urea derivatives **7a,b**.

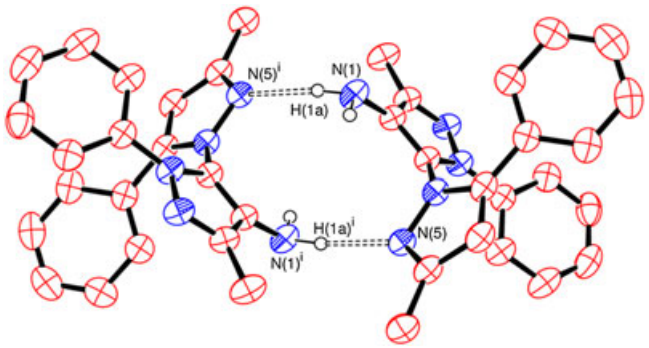

Fig. 6. ORTEP-3 view showing the intermolecular contact of a pair of atropisomers of **2d** thought hydrogen bonds. The displacement ellipsoids are shown at the 50% probability level. Hydrogen bonds are indicated by double dashed lines. Symmetry codes: $i = -x+2, -y+1, -z+1$.

a well-defined arrangement within the $P2_1/c$ lattice confirming the NMR and HPLC results. Figure 5 is an ORTEP-3[28] representation of the atropisomers that make up the crystallographic asymmetric, which was arbitrarily chosen to be the *aS*-atropisomer. It is important to note that *aS*- and *aR*-atropisomers form dimers related by the inversion symmetry and linked by two intermolecular symmetrically dependent hydrogen bonds (Fig. 6). These hydrogen bonds take place between the pyrazole nitrogen atom and the terminal amino group (N(1)–H(1a)...N(5)^{i}, symmetry code as in Figure 6. Considering the *aS*-atropisomer, the intramolecular geometry consists of four non-coplanar rings: two phenyl rings and two pyrazole ones. All of them are individually planar, including all the first neighbor atoms linked to them. Considering the non-H atoms, the largest deviations from the least-squares plane through the rings are 0.014(2), 0.002 (2), -0.006(1), and 0.004(2) Å, for A, B, C, and D, respectively (Fig. 5). The main intramolecular geometric parameters are given in Table S2 (see Supplementary Material). The two phenyl rings show the expected geometry with bond lengths and bond angles equivalents. On the other hand, the rings B and C present significant differences, mainly to N—N bonds: The difference between N(2)—N(3) and N(4)—N(5) is approximately 0.16 Å. These differences can be explained in terms of the electronic effects promoted by the amino group attached to pyrazole ring B. It is important to analyze the

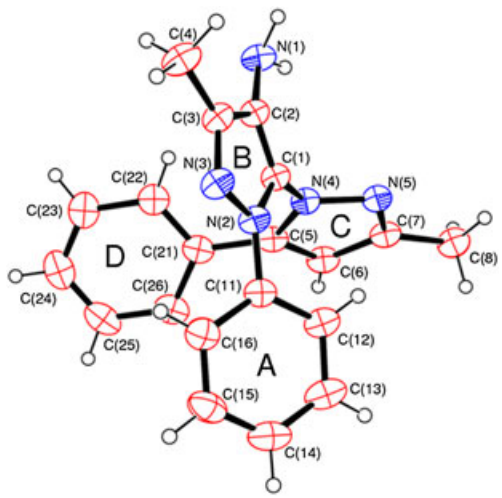

Fig. 5. ORTEP-3 view of **2d** (*aS*-atropisomer), showing the atom and ring labeling. The displacement ellipsoids are shown at the 50% probability level.

intramolecular geometry in terms of the dihedral angles between the rings. The angles formed between the least-square planes through A and B, B and C, and C and D rings are 34.2(1)°, 74.1(1)°, and 41.3(1)°, respectively. Considering the *aR*-atropisomer of **2d** in the racemic crystal, these values will be, as expected, -34.2(1)°, -74.1(1)°, and −41.3(1)°. Analyzing the intermolecular structure of **2d**, the dimers formed by pair of atropisomers are stacked along the direction through intermolecular nonclassic hydrogen bonds of the type H ... π-aryl involving the amine group hydrogen (donor) and the π acceptor of the D ring (Figure S1, see Supplementary Material). That means the H1b ... π-aryl$_{(\text{ring D})}$ hydrogen bonds contact the dimers through a translational symmetry along *a* axis. The final hydrogen bond geometry is shown in Table S3 (see Supplementary Material). In order to obtain the most realistic intermolecular geometry, the positional parameters of the two H atoms connected to the N atoms were not constrained during the refinements performed here. Our experimental data show that the dihedral angles between the NH_2 groups and the pyrazole ring plane are 59.82° and -10.64° for the H(1a)–N(1)–C(2)–C(3) and H(1b)–N(1)–C(2)–C(1) dihedral angles, respectively. Therefore, it is clear that the ideal planar geometry of the amino group is extremely affected by the packing conditions. Our experimental data show that the dihedral angles between the NH_2 groups and the pyrazole ring plane are 59.82 and -10.64° for the H(1a)–N(1)–C(2)–C(3) and H(1b)–(N1)–(C2)–(C1) dihedral angles, respectively.

Molecular Modeling

This study was undertaken to investigate rotational barrier energies around the dihedral angle (θ) defined in Figure 7 using HF/6-31G* level for single point energy calculations. The relative energies using $\theta = 180^{o}$ as a starting point (kcal/mol) for this calculation have been recorded, and the analysis of the plot of relative energy versus dihedral angle (Fig. 7) allowed us to identify two atropisomers of compound **2d**, in which the dihedral angle is approximately ±74° (Fig. 8). Both are separated by an energy barrier of approximately 41.11 kcal/mol (Fig. 7). Therefore, the calculations undertaken in this work support the existence of a high energy rotational barrier around the studied dihedral angle (θ), corroborating the existence of atropisomeric species of bipyrazole derivative **2d**. It is important to emphasize that the angles formed between the least-square planes through B and C rings in the X-ray analysis of the atropisomeric pair of **2d**, that is, 74.1(1)° and −74.1(1)° (Fig. 5), are

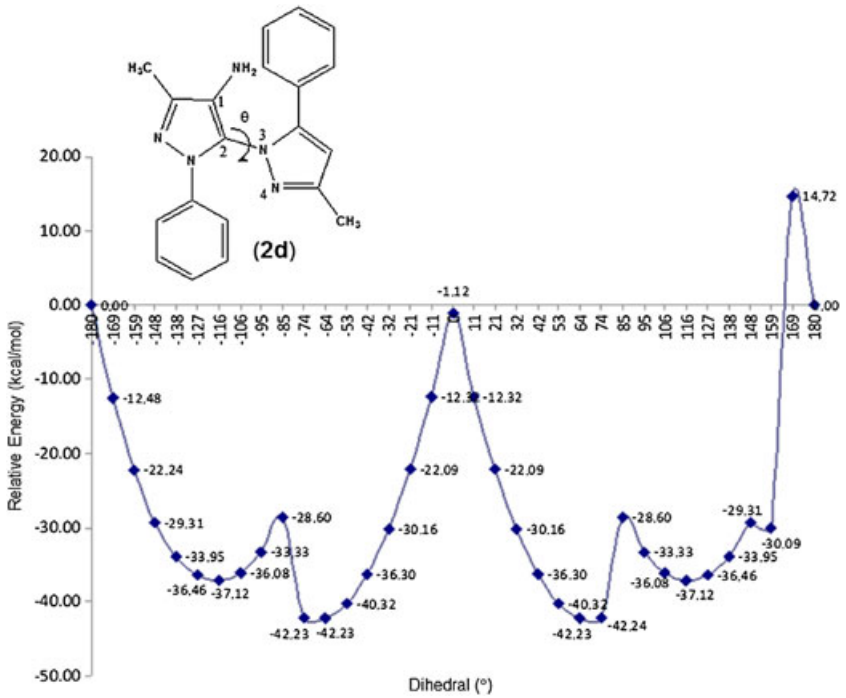

Fig. 7. Plot of relative energies versus dihedral angle (θ) of bipyrazole derivative **2d**.

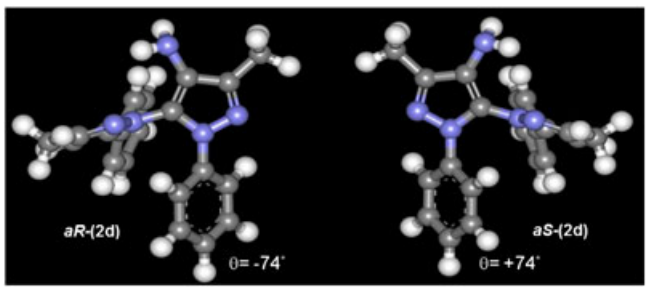

Fig. 8. Representation of more stable conformations of bipyrazole atropisomers **2d**.

in a perfect agreement with the dihedral angles obtained by molecular modeling studies.

CONCLUSIONS

We were able to confirm, by using different analytical techniques and molecular modeling tools, that the *ortho* bis-functionalized bipyrazole **2d** exists as a mixture of *aR*, *aS*-atropisomers. These results provide useful information to understand the pharmacological profile of this derivative and of several other 4-aminobipyrazole analogs.

ACKNOWLEDGMENTS

Special thanks are due to CAPES (BR.), CNPq (BR.), FINEP (BR.), and FAPERJ (BR.) for financial support and fellowships.

LITERATURE CITED

1. Smith WL, Meade EA, DeWitt DL. Pharmacology of prostaglandin endoperoxide synthase isozymes-1 and -2. Ann N Y Acad Sci 1994;714:136–142.
2. Smith WL, Lecomte M, Laneuville O, Breuer DK, DeWitt DL. Differential inhibition of human prostaglandin endoperoxide H synthases-1 and -2 by aspirin and other nonsteroidal anti-inflammatory drugs. Eur J Med Chem 1995;30(Suppl):417–427.
3. Rodrigues CR, Veloso MP, Fraga CAM, Miranda ALP, Barreiro EJ. Selective PGHS-2 inhibitors: a rational approach for treatment of the inflammation. Curr Med Chem 2002;9:849–867.
4. Penning TD, Talley JJ, Bertneshaw SR, Carten JS, Collins PW, Docter S, Graneto MJ, Lee LF, Malecha JW, Miyashiro JM, Rogers RS, Rogier DJ, Yu SS, Anderson GD, Burton EG, Cogburn JN, Gregory SA, Koboldt CM, Perkins WE, Seibert K, Veenhuizen AW, Zhang YY, Isakson PC. Synthesis and biological evaluation of the 1,5-diarylpyrazole class of cyclooxygenase-2 inhibitors: identification of 4-[5-(4-methylphenyl)-3-(trifluoromethyl)-1*H*-pyrazol-1-yl]benzenesulfonamide (SC-58635, Celecoxib). J Med Chem 1997;40:1347–1365.
5. Wu K. Biochemical pharmacology of nonsteroidal anti-inflammatory drugs. Biochem Pharmacol 1998;55:543–547.
6. Wallace JL, Chin BC. New generation NSAIDs. The benefits without the risks? Drugs Today 1997;33:371–378.
7. Davies NM, Jamali F. COX-2 inhibitors and cardiac toxicity: getting to the heart of the matter. J Pharm Pharmaceut Sci 2004;7:332–336.
8. Veloso MP. PhD Thesis, Chemistry Institute, Federal University of Rio de Janeiro, Rio de Janeiro, Brazil, 2000.
9. Santos AR, Pinheiro AC, Sodero ACR, Cunha AS, Padilha MC, Sousa PM, Fontes SP, Veloso MP, Fraga CAM. Atropisomerism: the effect of the axial chirality in bioactive compounds. Quim Nova 2007;30:125–135.
10. LaPlante SR, Edwards PJ, Fader LD, Jakalian A, Hucke O. Revealing atropisomer axial chirality in drug discovery. ChemMedChem 2011;6:505–513.
11. Enraf-Nonius. COLLECT. Nonius BV, Delft, The Netherlands; 1997–2000.
12. Otwinowski Z, Minor W. Processing of X-ray diffraction data collected in oscillation mode. In: Carter Jr. CW, Sweet RM, editors. Methods in enzymology. New York: Academic Press; 1997. p. 307–326.
13. Blessing RH. An empirical correction for absorption anisotropy, Acta Cryst 1995;A51:33–38.
14. Sheldrick GM. SHELXL-97. software for crystal structures analysis. Göttingen, Germany: Univ. of Göttingen; 1997.
15. Sheldrick GM. SHELXS-97. software for crystal structure resolution. Göttingen, Germany: University of Göttingen; 1997.
16. Parker D. NMR determination of enantiomeric purity. Chem Rev 1991;91:1441–1457.
17. Dewar MJS, Zoebisch EG, Healy EF, Stewart JJP. Development and use of quantum mechanical molecular models. 76. AM1: a new general purpose quantum mechanical molecular model. J Am Chem Soc 1985;107:3902–3909.

18. Spartan '08; Wavefunction, Inc. 18401 Von Karman Avenue, Suite 370. Irvine, California 92612, USA.
19. Hariharan PC, Pople JA. The influence of polarization functions on molecular orbital hydrogenation energies. Theor Chim Acta 1973;28:213–222.
20. Khan MA, Freitas ACC. Hetarylpyrazoles. IV. Synthesis and reactions of 1,5-bipyrazoles. J Heterocyclic Chem 1983;20:277–279.
21. Silveira AFB, Paulo LG, Miranda ALP, Rocha SO, Freitas ACC, Barreiro EJ. New pyrazolylhydrazone derivatives as inhibitors of platelet aggregation. J Pharm Pharmacol 1993;45:646–649.
22. Barreiro EJ, Camara CA, Verli H, Brazil-Más L, Castro NG, Cintra WM, Aracava Y, Rodrigues CR, Fraga CAM. Design, synthesis, and pharmacological profile of novel fused pyrazolo[4,3-*d*]pyridine and pyrazolo[3,4-*b*][1,8] naphthyridine isosteres: a new class of potent and selective acetylcholinesterase inhibitors. J Med Chem 2003;46:1144–1152.
23. Lages AS, Silva KCM, Miranda ALP, Fraga CAM, Barreiro EJ. Synthesis and pharmacological evaluation of new flosulide analogues, synthesized from natural safrole. Bioorg Med Chem Lett 1998;8:183–188.
24. Rothchild R. NMR methods for determination of enantiomeric excess. Enantiomer 2000;5:457–471.
25. Wolf C, Pranatharthiharan L, Volpe EC. A convenient method for the determination of the absolute configuration of chiral amines. J Org Chem 2003;68:3287–3290.
26. Cianci M, Helliwell JR, Helliwell M, Kaucic V, Logar NZ, Mali G, Tusar NN. Anomalous scattering in structural chemistry and biology. Crystallogr Rev 2005;11:245–335.
27. Flack HD. Chiral and achiral crystal structures. Helv Chim Acta 2003;86:905–921.
28. Farrugia LJ. ORTEP-3 for Windows—a version of *ORTEP*-III with a graphical user interface (GUI). J Appl Cryst 1997;30:565.